

Prospects to attain room temperature superconductivity

X. H. Zheng^{1,*}, J. X. Zheng², and D. G. Walmsley¹

¹*Department of Physics, Queen's University of Belfast, BT7 1NN, N. Ireland and*

²*Department of Electrical and Electronic Engineering, Imperial College London, SW7 2AZ, England*
(Dated: May 27, 2019)

With a generic model for the electron-phonon spectral density, two simple expressions are derived to estimate the transition temperature and gap-to-temperature ratio in conventional superconductors. They entail that on average the numerical value of the phonon exchange factor, λ , is limited to 2.67, so that room temperature superconductivity may be attained only with a Debye temperature of about 1800 K or higher, in materials that may or may not involve hydrogen. They also show that a Be-Pb alloy may become a superconductor at ~ 44 K.

PACS numbers: Analytic formulae, Transition temperature, Superconductivity

I. INTRODUCTION

In 1968 Ashcroft suggested that metallic hydrogen can be a high-temperature superconductor [1]. In 2004 Ashcroft suggested that hydrogen dominant metallic alloys in diamond anvil cells can become high-temperature superconductors at pressures considerably lower than may be necessary for metallic hydrogen [2]. In 2015 Eremets and co-workers indeed observed that sulfur hydride in a diamond anvil cell becomes a superconductor at 203 kelvin at about 150 GPa [3, 4]. Here we attempt to clarify whether the prospect of room temperature superconductivity is achievable in principle. We also demonstrate that, via virtual crystal approximation, a Be-Pb alloy may become a superconductor at ~ 44 K.

II. THEORY

We wish to find a general relation between the superconducting transition temperature, T_c , and other properties of the material, including the phonon exchange factor, λ , and Debye temperature, T_D , from numerical solutions to the Eliashberg equations. We apply the following generic model to evaluate the equations:

$$\alpha^2 F(\nu) = \lambda \nu^2 / (k_B T_D)^2, \quad \text{if } \nu \leq k_B T, \quad (1)$$

otherwise $\alpha^2 F(\nu) = 0$, where k_B is the Boltzmann constant, and ν the phonon frequency in joule or eV, see the Appendix for a justification. It is also consistent with the definition of λ [5] because, when we integrate $2\alpha^2 F(\nu)/\nu$ over ν , we simply recover the value of λ . In Eq. (1) the values of λ and T_D embody all phonon properties, leaving no ambiguities to our discussion within its premise.

In Eq. (1) T_D , if not available, can be replaced by the characteristic temperature, Θ , in the Bloch-Grüneisen formula for electrical resistivity, which is usually close to T_D , where $\Theta = 1223$ K in H_3S , found from Eq. (A4)

and FIG. S3 in [4] via numerical fitting. We also let the Coulomb pseudopotential $\mu^* = 0.09, 0.13$ and 0.17 , a usual range encountered experimentally [6, 7]. We will let $T = T_c$ once $\Delta(T) = 0.1\Delta_0$ instead of $\Delta(T) = 0$ [5]. This amounts to a new and just as accurate definition of T_c , because $\Delta(T)$ vanishes quickly as soon as it reaches $0.1\Delta_0$ with increasing T , a fact well known from the exemplary $\Delta(T)$ curve in [10].

III. RESULTS

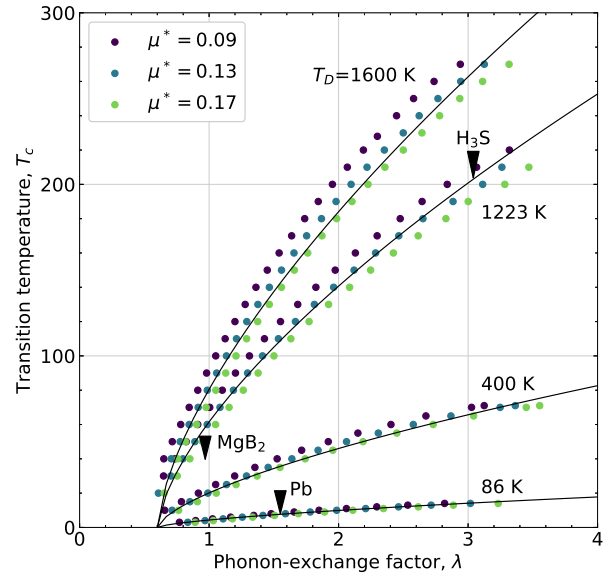


FIG. 1: Transition temperatures (dots) from the generic model in Eq. (1) against λ , $\mu^* = 0.09, 0.13$ and 0.17 (colour coded on line), $T_D = 86, 400, 1223$ and 1600 K. Experimental data for Pb, MgB_2 and H_3S are marked by downward black arrow heads. The curves are from Eq. (2).

We are now adequately equipped to solve the Eliashberg equations. Usually the procedure starts with a destination value of Δ_0 , giving T_c after the procedure terminates [11]; we instead start with a destination value

*Electronic address: xhz@qub.ac.uk

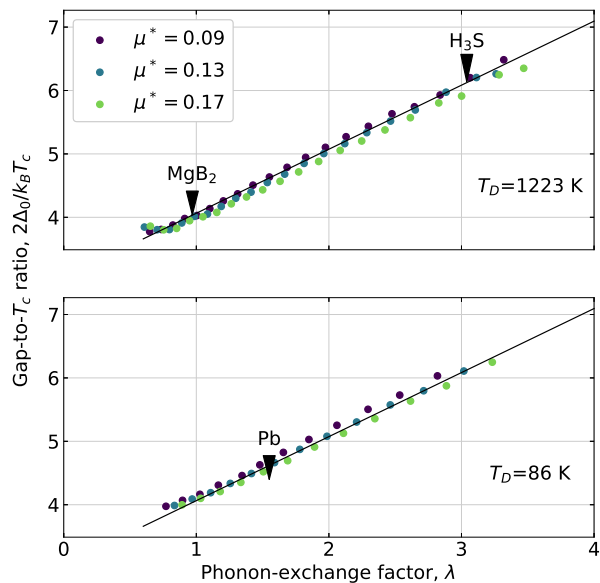


FIG. 2: Gap-to- T_c ratio, $2\Delta_0/k_B T_c$ (dots), from the generic model in Eq. (1), against λ , $\mu^* = 0.09, 0.13$ and 0.17 (colour coded on line), $T_D = 86$ (lower) and 1223 K (upper). Data for Pb, MgB₂ and H₃S are marked by downward black arrow heads. The lines are from Eq. (3).

of T_c . With given values of T_D and μ^* , we find λ via an optimization program of two dimensional search. In one dimension we search T to let the Eliashberg equations produce $\Delta(T) = 0.1\Delta_0$. In the other dimension we search λ until $|T - T_c| \sim 10^{-7}$ K. Meanwhile Δ_0 keeps evolving until our procedure terminates.

Our results, shown as dots in FIG. 1, align themselves into narrow bands, largely regardless of the values of μ^* . In particular, when $T_D = 86$ and 400 K, the dots appear to move along the same curve, in response to the varying values of μ^* — we therefore have an expression for T_c in terms of only λ and T_D , without involving μ^* but still retaining reasonable accuracy. We find the following power law relationship from numerical fitting

$$T_c = 0.23 T_D \left(0.25 \lambda - 0.15 \right)^{0.66} \quad (2)$$

which is applicable when $\lambda \geq 0.6$. We also find the following linear relationship

$$\frac{2\Delta_0}{k_B T_c} = 4.04 \left(0.25 \lambda - 0.15 \right) + 3.66 \quad (3)$$

which is likewise applicable when $\lambda \geq 0.6$. Outcomes of Eqs. (2) and (3) are shown as curves and lines in FIGs. 1 and 2 respectively.

We always encounter an upper limit of λ in our numerical procedure. For example, at $T_D = 400$ K, our numerical procedure fails to converge once $\lambda > 2.57$, or $T_c > 77$ K, which we will refer to as the observed maximum value of the transition temperature (possible reasons discussed in Section VI). In FIG. 3 we plot the

TABLE I: SUPERCONDUCTOR PARAMETERS

Matter	T_D^a	T_c^a	λ^b	$2\Delta_0/k_B T_c^b$
V	380	5.38	0.66 (0.81)	3.72 (3.40)
Sn	200	3.72	0.69 (0.72)	3.75 (3.50)
Ta	240	4.48	0.69 (0.69)	3.75 (3.60)
In	108	3.40	0.80 (0.81)	3.86 (3.60)
Nb	275	9.50	0.83 (0.97)	3.89 (3.80)
MgB ₂ ^c	815	39.0	0.97 (0.92)	4.03 (4.02)
Hg	71.9	4.16	1.09 (1.62)	4.16 (4.60)
Pb	105	7.19	1.24 (1.55)	4.30 (4.38)
Li ^c	147	14.9	1.76 (NA)	4.83 (NA)
H ₃ S ^c	1223	203	3.04 (NA)	6.12 (NA)

^aFrom [16] unless stated otherwise.

^bCalculated or directly from [7, 14–16] (bracketed).

^cCalculated, T_c from [3, 13, 14].

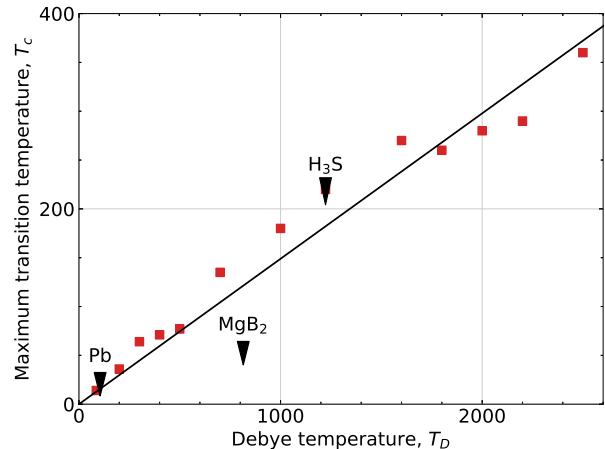


FIG. 3: Observed maximum values of T_c (in kelvin, filled squares) and T_c in Pb, MgB₂ and H₃S (downward arrow heads) against T_D . The line is from Eq. (2) with $\lambda = 2.67$.

empirical maximum values of T_c (filled squares) found at $86 \leq T_D \leq 2500$ K. We also plot a line for T_c from Eq. (2), with $\lambda = 2.67$ to ensure a minimum r.m.s. difference between the output of the formula and values of the observed maximum T_c .

In TABLE 1 the values of T_D in dense Li and H₃S are replaced by the Bloch-Grüneisen characteristic temperatures [12] we extracted from the electrical resistance data in [3, 13]. MgB₂ is a two band superconductor, with two values of Δ_0 , and we evaluate $2\Delta_0/k_B T_c$ with the larger Δ_0 [14]. The experimental λ in MgB₂ is an average between its values in the σ and π bands [15]. The theoretical λ is calculated from Eq. (2) with experimental T_D and T_c . The theoretical gap-to- T_c ratios are from Eq. (3) with theoretical λ .

To the best of our knowledge experimental values of λ and $2\Delta_0/k_B T_c$ in dense Li and H₃S are not yet available. According to Errea and co-workers $\lambda = 2.64$ or 1.84 for harmonic or anharmonic phonons respectively in H₃S in theory, with $\Delta_0 \approx 43$ meV and $T_c = 190$ K ($\mu^* = 0.16$, anharmonic phonons) giving $2\Delta_0/k_B T_c \approx 5.25$ [17], com-

pared with λ between 2.07 and 2.19 in $(\text{H}_2\text{S})_2\text{H}_2$ in theory [18], largely consistent with our results considering the many uncertainties in theoretical evaluations.

IV. MCMILLAN FORMULA

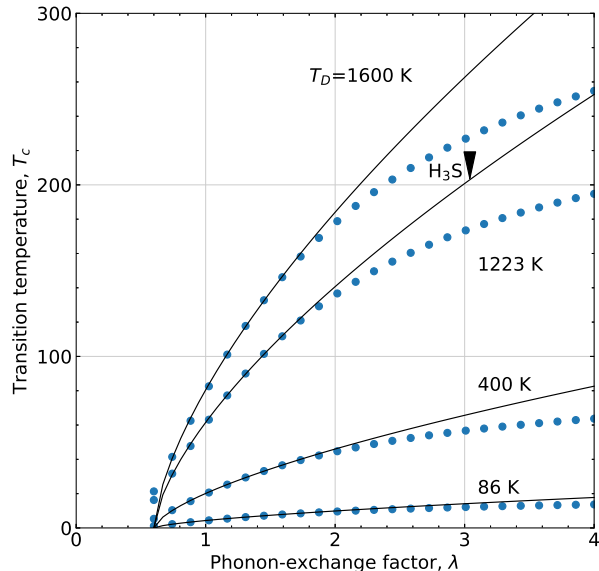


FIG. 4: Comparison between transition temperatures from Eq. (2) (curves) and Eq. (4) (dots, $\mu^* = 0.13$).

In 1968 McMillan [5] solved the Eliashberg equations via iteration with a number of simplifications. The equations are linearised at $T = T_c$, the solutions are assumed to have just two values, Δ_0 and Δ_∞ , defined immediately beneath the surface and deeply inside of the Fermi sphere, respectively, and $\alpha^2 F(\nu) = \alpha^2 \times F(\nu)$, α being a constant and $F(\nu)$ the phonon density of states (from Nb neutron scattering experiment for any bcc lattice, assumed to vanish below 8.6 meV). During the iteration T_c and μ^* are kept constant, α adjusted continuously to keep Δ_0 constant. The formula

$$T_c = \frac{T_D}{1.45} \exp \left[-\frac{1.04(1 + \lambda)}{\lambda - \mu^*(1 + 0.62\lambda)} \right] \quad (4)$$

results from numerical fitting, and has proven to be highly successful in guiding both theoreticians and experimentalists. For clarity we choose $\mu^* = 0.13$ and plot the outcome of Eq. (4) in FIG. 4 as dots, which matches the outcome of Eq. (2) closely if $\lambda < 2$, but otherwise underestimates T_c , rather significantly in the parameter region of H_3S .

In 1975 Allen and Dynes [6] published a slightly modified T_c formula where $T_D/1.45$ in Eq. (4) is replaced by $\omega_{\text{ln}}/1.2$, $\omega_{\text{ln}} = (2/3)T_D$ with our generic model in Eq. (1) in place, that is T_c from Eq. (4) will be suppressed by $\sim 20\%$. In 1984 Mitrović, Zarate and Carbotte [7] found

an approximate formula for $2\Delta_0/k_B T_c$ in terms of T_c/ω_{ln} , not directly comparable with Eq. (3).

V. BERYLLIUM-LEAD ALLOY

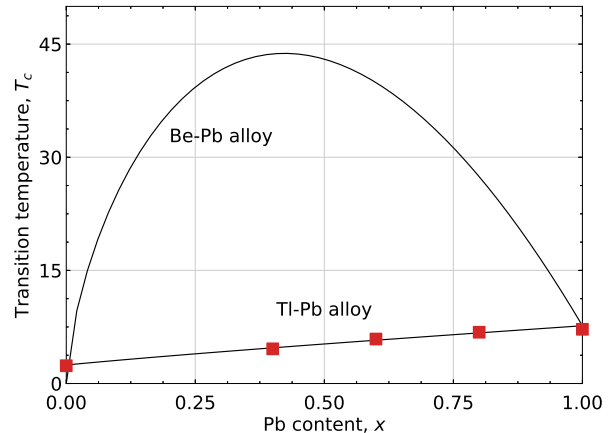


FIG. 5: Transition temperatures in Tl-Pb alloys. The dots are experimental data and the curves are theoretical calculations from Eq. (2) with the virtual crystal approximation.

Eqs. (2) and (3) enable us to predict superconductivity quantitatively, not only in simple metals but also in alloys. For example, in Pb we have $T_D \simeq \Theta_1 = 86$ K (Bloch-Grüneisen characteristic temperature) and $\lambda = \lambda_1 = 1.55$, giving $T_c = 7.66$ K via Eq. (2), compared with an empirical value of 7.19 K [7]. In Tl we have $T_D = \Theta_2 = 78.5$ K [16] and $\lambda = \lambda_2 = 0.795$, giving $T_c = 2.46$ K, compared with the empirical 2.36 K [7]. Letting $T_D = x\Theta_1 + (1-x)\Theta_2$ and $\lambda = x\lambda_1 + (1-x)\lambda_2$, where x is the content of Pb in a Tl-Pb alloy in accordance with the well-established virtual crystal approximation [19], we find T_c in the alloys from Eq. (2) with r.m.s. deviation = 4.2% against experimental data, as is shown in FIG. 5 and TABLE 2.

TABLE II: THALLIUM-LEAD ALLOY PROPERTIES^a

Pb	Tl	Θ	λ	T_c^b
0.0	1.0	78.5	0.795	2.46 (2.36)
0.4	0.6	81.5	1.097	4.73 (4.60)
0.6	0.4	83.0	1.248	5.74 (5.90)
0.8	0.2	84.5	1.399	6.71 (6.80)
1.0	1.0	86.0	1.550	7.66 (7.19)

^aFrom virtual crystal approximation.

^bExperimental values from [7] (bracketed).

Replacing Tl with Be allows us to now make a prediction for T_c in Be-Pb alloys, by applying the same virtual crystal approximation. With $\Theta_3 = 1440$ K (Debye temperature) and $\lambda_3 = 0.6$ to let $T_c \sim 0$ ($= 0.026$ K in reality) for Be [16], we let $T_D = x\Theta_1 + (1-x)\Theta_3$ and

$\lambda = x\lambda_1 + (1-x)\lambda_3$. This leads through Eq. (2) to give the upper curve in FIG. 5, where the value of T_c reaches a peak of 43.8 K.

VI. DISCUSSION

Eqs. (2) and (3) entail a few interesting physical consequences. First, there must be an upper limit of λ . If $\lambda \gg 1$ then we have $\Delta_0 \sim 0.51\lambda k_B T_c$ from Eq. (3), and this leads through Eq. (2) to $\Delta_0 \sim 0.47\lambda^{1.66} k_B T_D$. Consequently we have $\Delta_0/\lambda k_B T_D \sim 0.47\lambda^{0.66} \rightarrow \infty$ when $\lambda \rightarrow \infty$. This is impossible, because Δ_0 is the edge of superconducting energy gap function, whereas $\lambda k_B T_D$ measures the strength of the electron-phonon interactions, the underlying reasons for superconductivity to arise, and the two must be compatible. This explains why in FIGs. 1, 2 and 3 the numerical values of λ are limited to 2.67 on average.

It is remarkable that McMillan also found a value of λ in association with maximum T_c [5]. He argued that in Eq. (4) $T_D \sim \langle \omega \rangle$ and $\lambda \sim 1/\langle \omega^2 \rangle$, where ω stands for phonon frequency, so that $T_c \rightarrow 0$ when $\langle \omega \rangle$ is either too large or too small. Searching for maximum T_c leads to $\lambda = 2$, not far from our value 2.67. He estimated T_c may reach 9.2 K for lead-based alloys and 40 K for V₃Si [5]. It appears that T_c in the BCS theory is indeed curbed by an intrinsic limit, which cannot be lifted by strong electron-phonon interactions, reminiscent of the speed limit imposed by the Lorentz transformation.

Second, it is immediately apparent from Eq. (2) that, with $\lambda \sim 2.67$, the only realistic try for us to achieve high T_c is in materials with high T_D . Indeed we know from TABLE I that in MgB₂ we have $T_c = 39$ K with $\lambda = 0.97$ and $T_D = 815$ K, compared with $T_c = 7.19$ K, $\lambda = 1.24$ but $T_D = 105$ K in Pb. If somehow we were able to let $\lambda = 2.67$ in both cases, then in MgB₂ we would have $T_c = 121$ K from Eq. (2), compared with $T_c = 16$ K in Pb. Indeed, it is clear from FIG. 1 that, ascending along the T_c curves with $T_D = 86$ or 400 K, there is hardly any hope for us to reach $T_c \sim 300$ K.

Third, we might be able to push T_c into the range of room temperatures, but just barely. We know from TABLE I that we may have $\lambda = 3.04$, and this leads through Eq. (2) to $T_c = 300$ K with $T_D \sim 1800$ K. From direct numerical calculation we find $T_c = 255$ K with $\lambda = 2.39$ and $T_D = 1800$ K. Whether or not we can achieve higher T_c with some $\alpha^2 F(\nu)$ other than the generic model in Eq. (1) remains an open question, but we suspect the potential is rather limited, unless $T_D \sim 2500$ K or higher were an option at our disposal.

Finally, the close fit between the dots and the lower curve in FIG. 5 tells us that T_c , from Eq. (2), in virtual crystal approximation, is trustworthy in the case of the Tl-Pb alloys. If the higher curve in FIG. 5 is just as accurate, we may achieve $T_c \sim 44$ K in Be-Pb alloys, due to Fermi surface enlargement, on account of the large valence in Pb (= 4). The Be-Bi alloy may also be worth

considering because Bi, though not a superconductor in bulk form, was proven to be highly effective to raise T_c in Pb-Bi alloys [7] apparently likely due to its very large valance (= 5).

VII. CONCLUSIONS

We conclude with suggestions for future work. We wish for the experimental values of λ and $2\Delta_0/k_B T_c$ in dense lithium and H₃S to be made available, to validate or dispute our theoretical predictions in TABLE I. In the periodic table T_D can reach 1440 and 2230 K in beryllium and carbon respectively [16] formally nearly or more than enough for $T_c \sim 300$ K with $\lambda \sim 3$. Indeed $T_c = 18$ K in potassium-doped C₆₀ [20]. It would be interesting to see what will happen in beryllium, doped with lead or other metals to become an alloy with an enlarged Fermi surface. Experimentally this may be achieved via the vacuum-sputtering technique [21] to make a uniform film of an alloy of two or more metals or, if necessary, a pancake film of multiple layers of different atoms.

APPENDIX

Here we justify Eq. (1) in the main text. By definition

$$\alpha^2 F(\nu) = \frac{1}{N} \sum_{\ell, \mathbf{q}} \delta(\nu - \hbar\omega_\ell) \delta(\epsilon - \epsilon_F) |g_\ell(\mathbf{q})|^2 \quad (\text{A1})$$

for a spherical Fermi surface, where ℓ identifies phonon polarization, N is the number of atoms per unit volume, \mathbf{q} and $\omega_\ell = \omega_\ell(\mathbf{q})$ phonon momentum and frequency, \mathbf{k} and $\epsilon = \epsilon(\mathbf{k})$ electron momentum and energy, ϵ_F Fermi energy, and $g_\ell(\mathbf{q})$ matrix element [22]. In the normal state

$$\alpha_{\text{tr}}^2 F(\nu) = \frac{1}{N} \sum_{\ell, \mathbf{q}} \delta(\nu - \hbar\omega_\ell) \delta(\epsilon - \epsilon_F) |g_\ell(\mathbf{q})|^2 \times \left[\frac{\mathbf{k} \cdot (\mathbf{k} + \mathbf{q})}{\mathbf{k} \cdot \mathbf{k}} - 1 \right] \quad (\text{A2})$$

and its model

$$\alpha_{\text{tr}}^2 F(\nu) = \begin{cases} \lambda_{\text{tr}}(\nu/k_B\Theta)^4, & \nu \leq k_B\Theta \\ 0, & \text{otherwise} \end{cases} \quad (\text{A3})$$

lead through relevant formulations [23] to the Bloch-Grüneisen formula

$$\frac{\rho(T)}{\rho(\Theta)} = 4.2263 \left(\frac{T}{\Theta} \right)^5 \int_0^{\Theta/T} \frac{x^5 dx}{(e^x - 1)(1 - e^{-x})} \quad (\text{A4})$$

where $\rho(T)$ and $\rho(\Theta)$ are electrical resistivity measured at T and Θ , respectively, Θ being the characteristic temperature, highly accurate in most metals over a broad

range of temperatures [12]. If the sound velocity is constant anywhere within the first Brillouin zone in reciprocal space (Debye model) then

$$\frac{\mathbf{k} \cdot (\mathbf{k} + \mathbf{q})}{\mathbf{k} \cdot \mathbf{k}} - 1 \propto \left(\frac{\nu}{k_B \Theta} \right)^2 \quad (\text{A5})$$

for normal phonons. Assuming that Eq. (A5) also applies to umklapp phonons, that is assuming the size of the phonon sphere is always proportionally measured by the

value of phonon frequency (energy), we find Eq. (1) via Eqs. (A1–A3).

ACKNOWLEDGEMENTS

The authors wish to thank Professor Nikolay Plakida for useful discussions.

-
- [1] N. W. Ashcroft, *Phys. Rev. Lett.* **21** (1968) 1748.
 [2] N. W. Ashcroft, *Phys. Rev. Lett.* **92** (2004) 187002.
 [3] A. P. Drozdov, M. I. Erements, I. A. Troyan, V. Ksenofontov, S. I. Shylin, *Nature* **525** (2015) 73.
 [4] F. Capitani, B. Langerome, J.-B. Brubach, P. Roy, A. Drozdov, M. I. Erements, E. J. Nicol, J. P. Carbotte, T. Timusk, *Nature Phys.* **13** (2017) 859.
 [5] M. I. McMillan, *Phys. Rev.* **167** (1968) 331.
 [6] P. B. Allen, R. C. Dynes, *Phys. Rev. B* **12** (1975) 905.
 [7] B. Mitrović, H. G. Zarate, J. P. Carbotte, *Phys. Rev. B* **29** (1984) 184.
 [8] C. R. Leavens, *Phys. Rev. B* **29** (1984) 5178.
 [9] X. H. Zheng, D. G. Walmsley, *Phys. Rev. B* **77** (2008) 104510.
 [10] J. Bardeen, L. N. Cooper, J. R. Schrieffer, *Phys. Rev.* **108** (1957) 1175.
 [11] W. McMillan, J. M. Rowell, *Phys. Rev. Lett.* **14** (1965) 108.
 [12] J. M. Ziman, *Electrons and phonons*, Clarendon, Oxford, 2001.
 [13] K. Shimizu, H. Ishikawa, D. Takao, T. Yagi, K. Amaya, *Nature* **419** (2002) 597.
 [14] T. Masui, K. Yoshida, S. Lee, A. Yamamoto, S. Tajima, *Phys. Rev. B* **65** (2002) 214513.
 [15] O. V. Dolgov, R. S. Gonnelli, G. A. Ummarino, A. A. Golubov, S. V. Shulga, J. Kortus, *Phys. Rev. B* **68** (2003) 132503.
 [16] C. Kittel, *Introduction to solid state physics*, John Wiley, New York, 1986.
 [17] I. Errea, M. Calandra, C. J. Pickard, J. Nelson, R. Needs, Y. Li, H. Liu, Y. Zhang, Y. Ma, F. Mauri, *Phys. Rev. Lett.* **114** (2015) 157004.
 [18] D. Duan, Y. Liu, D. Li, X. Huang, Z. Zhao, H. Yu, B. Liu, W. Tian, T. Cui, *Sci. Rep.* **4** (2014) 6968.
 [19] von L. Nordheim, *Ann. Phys. (Leipzig)* **9** (1931) 607.
 [20] A. F. Hebard, M. J. Rosseinsky, R. C. Haddon, D. W. Murphy, S. H. Glarum, T. T. M. Palstra, A. P. Ramirez, A. R. Kortan, *Nature* **350** (1991) 600.
 [21] A. Inam, M. S. Hegde, X. D. Wu, T. Venkatesan, P. England, P. F. Miceli, E. W. Chase, C. C. Chang, J. M. Tarascon, J. B. Wachtman, *Appl. Phys. Lett.* **53** (1988) 908.
 [22] P. T. Truant, J. P. Carbotte, *Can. J. Phys.* **52** (1974) 618.
 [23] P. G. Tomlinson, J. P. Carbotte, *Can. J. Phys.* **55** (1977) 751.